Journal of Alloys and Compounds 617 (2014) 81–85

Contents lists available at ScienceDirect

Journal of Alloys and Compounds

journal homepage: www.elsevier.com/locate/jalcom

Effect of Al content on structure and properties of TiAlCN coatings prepared by magnetron sputtering

Xuhai Zhang [a,b], Yuedong Qiu [a], Zheng Tan [a], Jianliang Lin [b,c], Aiqun Xu [a], Yuqiao Zeng [a,*], J.J. Moore [b], Jianqing Jiang [a]

[a] *Jiangsu Key Laboratory of Advanced Metallic Materials, School of Materials Science and Engineering, Southeast University, Nanjing 211189, China*

[b] *Advanced Coatings and Surface Engineering Laboratory (ACSEL), Colorado School of Mines, 1500 Illinois Street, Golden, CO 80401, USA*

[c] *Surface Engineering & Materials Chemistry, Materials Engineering Dept., Mechanical Engineering Division, Southwest Research Institute, 6220 Culebra Road, San Antonio, TX 78238-5166, USA*

ARTICLE INFO

Article history:
Received 27 March 2014
Received in revised form 29 July 2014
Accepted 1 August 2014
Available online 10 August 2014

Keywords:
Coating materials
Nitride materials
Vapor deposition
Mechanical properties
Microstructure

ABSTRACT

TiAlCN coatings were deposited by direct current reactive magnetron co-sputtering. In the coatings, the (Al + Ti), C and N contents were kept constant and the Al content is varied according to the different Al/Ti target power ratio. The structure, mechanical and tribological properties of the TiAlCN coatings were strongly depended on the Al content. Even a small amount of Al addition led to the notable precipitation of hcp-AlN in fcc-TiN matrix. However, only a proper amount of Al content resulted in a significant refinement of the coating structure. The refined structure composed of fcc-TiN and hcp-AlN crystals with a size of 10–20 nm exhibited a unique combination of high hardness and low friction coefficient.

1. Introduction

Hard coatings have been widely applied on surfaces of various cutting and forming devices to reduce their wear or corrosion. The operating life of the tools can thus be significantly extended. The binary TiN coating prepared by physical vapor depositions (PVD) or chemical vapor depositions (CVD) is one of the most extensively used protective coatings [1–4]. Although it exhibits high wear resistance, the TiN coating does not provide sufficient protection in some cases. For instance, the hardness and oxidation resistance decrease dramatically when the TiN coating is subjected to high-speed cutting with lubricant free [5,6]. Meanwhile, the coefficient of friction (COF) is not satisfactory and the toughness is relatively low [7,8]. With the aim of overcoming these shortcomings, different elements are introduced into the TiN coatings to form new systems. Among them, the ternary TiAlN coating shows high corrosion resistance [9] and the TiCN coating exhibits low COF [7]. Therefore it is expected that a quaternary TiAlCN coating may display a unique combination of high thermal stability and outstanding tribological properties. The recent research proves that the TiAlCN coatings possess enhanced performance in comparison with the TiN, TiAlN and TiCN coatings. However, most of these work focuses on the effect of carbon content on the structure and properties of the TiAlCN coatings since carbon can exist in various forms, such as hard nanocrystalline compounds or amorphous lubricants [10–14] which result in highly tunable coating structures and properties. There are also several reports on the effect of N content in TiAlCN coatings [15].Though it has been well documented that the Al content plays an important role in the structure and properties of TiAlN coatings [5,16,17], there are few investigations on the effect of the Al content on TiAlCN coatings.

In this work, TiAlCN coatings with different Al contents were deposited by reactive magnetron sputtering and the relationship among the Al content, coating structure, mechanical and tribological properties were discussed.

2. Material and methods

2.1. Coating deposition

TiAlCN coatings were deposited by reactive magnetron sputtering in a mixture of Ar and N_2 gases at a constant flow ratio of 7:3. The working pressure was 3 m Torr. Three targets, including pure graphite (99.99 %), Ti (99.99 %) and Al (99.99 %), with a diameter of 5 inch were supported by direct current (DC) power (Advanced Energy, 100 kHz) to provide Ti, Al and C elements to the TiAlCN coatings. The depositing power configuration was shown in Table 1, which guaranteed the constant N, C and (Ti + Al) contents in the as-obtained TiAlCN coatings, as well as

---

[*] Corresponding author. Tel.: +86 025 52090636.
E-mail address: zyuqiao@seu.edu.cn (Y. Zeng).

http://dx.doi.org/10.1016/j.jallcom.2014.08.009

Table 1
Depositing target power configuration.

Sample number	C1#	C2#	C3#	C4#	C5#
C target power (W)	350	450	450	450	450
Ti target power (W)	600	700	600	600	550
Al target power (W)	0	100	200	300	400
Al/Ti power ratio	0	0.14	0.33	0.50	0.73

a tunable Al content. Polished 304 stainless steel and (1 1 1) Si wafers were used as the deposition substrates. A Ti interlayer with a thickness of about 100 nm was applied on the substrates before the coating deposition to improve the adhesion between the coatings and the substrates.

2.2. Coating characterizations

The elemental compositions of the TiAlCN coatings were characterized by energy dispersive spectroscopy analyzer (EDS, FEI. Sirion 200). X-ray diffraction (XRD) using Cu Kα radiation was performed on the as-obtained coatings to investigate the phases. Raman spectra of the coatings were also studied using a HR-800 Raman spectrometer operated at a laser wavelength of 546 nm with 16mW output. The morphologies of the TiAlCN coatings were observed using scanning electron microscopy (SEM, FEI. Sirion 200) and transmission electron microscopy (TEM, FEI, Tecnai G2). TEM samples were prepared by electrolytic single jet thinning using a solution containing $HClO_4$ and C_2H_5OH.

The hardness of the coatings was tested by nanoindentation (STM nanoindenter XP). At least 10 measurements were performed on each coating. COF of the coatings was tested by ball on disc tribometer (CETR, Inc) at a sliding speed of 0.39 m/s. In the friction test, a WC-Co ball with a diameter of 1 mm was used as the counterpart with a load of 0.5 N on it.

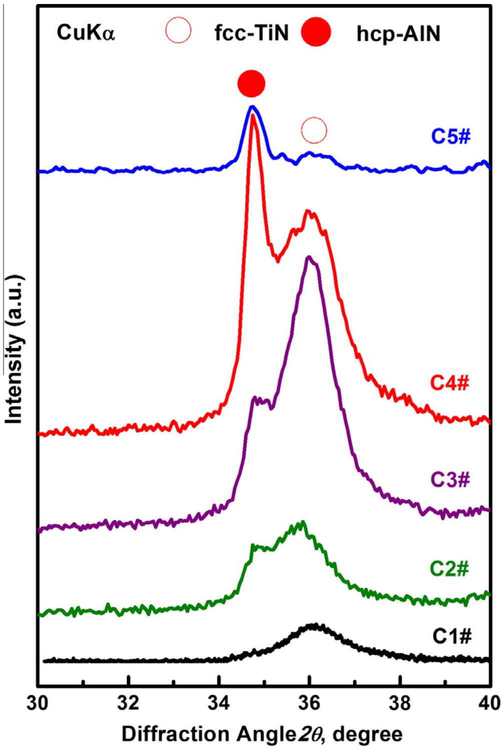

Fig. 1. XRD patterns of the TiAlCN coatings with different Al contents.

3. Results and discussion

3.1. Composition and structure of the TiAlCN coatings

In this work, the TiAlCN coatings prepared at the Al/Ti target power ratio of 0, 0.14, 0.33, 0.50 and 0.73 are named as C1#, C2#, C3#, C4# and C5#, respectively. The chemical compositions of these coatings are measured by EDS and the results are shown in Table 2. As the Al/Ti power ratio increases from 0 to 0.73, the Al content increases monotonically from 0 to 18 at.%, while the N, C and (Ti + Al) contents keep constant at about 32 at.%, 12 at.% and 56 at.%, respectively.

The phase evolution of the TiAlCN coatings as a function of the Al addition is followed in Fig. 1 by XRD. C1# contains a single fcc-TiN phase with a preferential orientation in (1 1 1) at the diffraction peak 2*θ* of about 36.05° [18,19].The fcc-TiN lattice parameter is slightly larger when compared with the ideal TiN phase (JCPDF-87-0663 TiN), since parts of the N atoms in the TiN lattice are replaced by C atoms with larger size in C1# [18,19]. With the increasing Al addition in the coatings, the (1 1 1) diffraction angle associated with the fcc-TiN phase decreases gradually. The replacement of Ti by Al in fcc-TiN contributes to the decrease. Different from the reported ternary TiAlN coatings [5,9], even a small amount of Al addition can cause the notable formation of hcp-AlN as evidenced by the arising diffraction peak at 2*θ* of about 34.83°, corresponding to the (0 0 2) of hcp-AlN [20]. It should be noticed that the (0 0 2) diffraction angle of the hcp-AlN formed in this study is much lower than that of the pure and stable hcp-AlN crystals. The similar phenomenon has been observed by Gago et al. [20]. They found that when the N content in the TiAlN coating was higher than 25 at.%, the (0 0 2) diffraction peak of the hcp-AlN made a remarkable shift towards lower angel values. The emergence of strain may contribute to this shift [20]. With the increasing Al content in the TiAlCN coatings, the diffraction intensity of hcp-AlN increases and finally the (0 0 2) of hcp-AlN becomes the dominant diffraction peak in C5#, suggesting an increasing hcp-AlN content in TiAlCN coatings. Using the Scherer formula, the crystal sizes of both fcc-TiN and hcp-AlN are estimated and summarized in Table 3. The most prominent grain refinement of fcc-TiN can be observed in C4#, where the smallest fcc-TiN crystals with a size of about 53 nm are obtained. In the case of hcp-AlN, the grain size exhibits an increasing tendency with the increasing Al addition.

The Raman spectra of the TiAlCN coatings with different Al contents are shown in Fig. 2, where the first-order transverse acoustic (TA), longitudinal acoustic (LA), transverse optical (TO) and the second-order acoustic (2A) mode of fcc-TiN, as well as the E_2 and A_1(LO) of hcp-AlN, are involved. In C1#, the TA, LA and TO of fcc-TiN can be detected except that the replacement of partial N by C in fcc-TiN leads to a peaks shift towards higher wave numbers, agreeing with the former report [21,22]. Usually, the ratio of acoustical to optical scattering intensities is a measure of the Ti: N atomic ratio in fcc-TiN phase [23]. In C1#, the intensity of the optical scattering peak (at about 600 cm^{-1}) is much higher than that of the acoustical scattering peak (at about 270 cm^{-1}), indicating that the fcc-TiN in C1# has an over-stoichiometric composition. Though

Table 2
Chemical compositions of the TiAlCN coatings (measured by EDS).

Sample number	C1#	C2#	C3#	C4#	C5#
N content (at.%)	28	33	32	32	35
C content (at.%)	18	12	13	13	12
Ti + Al content (at.%)	54	55	55	55	53
Ti content (at.%)	54	52	47	43	35
Al content (at.%)	0	3	8	12	18

Table 3
Crystal size of fcc-TiN and hcp-AlN calculated using the Scherer formula.

Crystal	C1#	C2#	C3#	C4#	C5#
fcc-TiN phase (nm)	61	67	71	53	133
hcp-AlN phase (nm)	0	105	126	187	183